Ring Cusp Discharge Chamber Performance Optimization

Jeffrey M. Hiatt* and Paul J. Wilbur†
Colorado State University, Fort Collins, Colorado

An experimental study of the effects of discharge chamber length and the location of the anode, cathode, and magnetic field ring cusp within the chamber on the performance of an 8-cm-diam ring cusp thruster is described. Performance changes are measured in terms of plasma ion energy costs, extracted ion fractions, and ion beam profiles. Results show that the anode may be positioned at any location along an "optimum virtual anode" magnetic field line, and minimum plasma ion energy costs will result. The actual location of this field line is related to a "virtual cathode" magnetic field line that is defined by the cathode position. The magnetic field has to be such that the virtual anode field line intersects the grids at the outermost ring of grid holes to maximize the extracted ion fraction and the ion beam profile flatness. Discharge chamber lengths that were as small as possible in the test apparatus yielded the highest extracted ion fractions.

Introduction

OVER the years, discharge chamber dimensions and magnetic field configurations and strengths have been altered in a continuing effort to improve ion thruster discharge chamber performance. The detailed mechanism by which such design alterations induce performance changes have, however, not been well understood. As a result it has been difficult to separate out the cause-and-effect relationships associated with each of the thruster design variables, and it has therefore not been possible to develop models that facilitate design of new thrusters without experimental optimization. Recently, however, both a model that enables one to describe discharge chamber performance in terms of two physically meaningful parameters (plasma ion energy cost and extracted ion fraction) and an experimental technique that can be applied to measure these parameters have been proposed.[1,2]

An objective of the work described herein has been to apply this experimental technique to determine the effects of changes in anode and cathode locations and magnetic field shape on these key performance parameters. A further objective has been to apply the discharge chamber model to infer the mechanisms by which such changes induce improvements in discharge chamber performance.

A small (8-cm-diam) thruster has been selected for this study because a small thruster should tend to perform more poorly than a larger one[2] and it was expected that the performance of a small thruster would be more sensitive to the geometric changes being investigated. The ring cusp discharge chamber design[3] was selected for the study because it shows substantial promise as a very efficient configuration for ion thruster applications.

Apparatus and Procedure

The side schematic view of the 8-cm-diam discharge chamber used in these studies is shown in Fig. 1a. A unique feature of this discharge chamber design is its loop anode, which can be move axially during operation (variable ℓ_a) by means of the lead screw, yoke, and guidepost assembly. This capability, coupled with the option of installing anode loops varying in diameter d_a from 4 to 6.6 cm, facilitates investigation of the effects of changes in the position of the anode relative to the magnetic ring cusp on the performance of a discharge chamber. The loop anode was selected for the study because its axisymmetric configuration and small cross section facilitate the definition of a small circular zone at which electrons are being extracted from the plasma.

While the various anode loops could be moved either upstream or downstream of the cusp location, preliminary tests[4] showed that performance was always best when they were moved downstream toward the grids. It is postulated that upstream anode movement gives poorer performance because it induces a greater fraction of the total ion production upstream of the cusp and the probability of an ion being extracted into the beam from this region is lower than the probability of extraction of an ion from a region closer to the grids. For the data presented herein, only anode positions downstream of the loop anode will be investigated and values of ℓ_a will be positive. The magnetic field for the thruster of Fig. 1a is produced by small samarium cobalt magnets placed end to end to form a ring located a distance ℓ_r upstream of the grids and the samarium cobalt upstream centerline magnet shown. These magnets have a flux density of 0.27 T at their surfaces, and they are arranged so that the polarity on the outer surface of the ring of magnets (or ring magnet) is opposite to that at the outer surface of the centerline magnet.

While most tests were run with the movable anode configuration of Fig. 1a, it was considered important to compare performance measurements made with this apparatus to those made with the anode located at the magnetic field cusp on the surface of the magnet. The ion source was modified for this comparative test by removing the anode loop, yoke, and lead screw of Fig. 1a and installing the thin sheet steel anode adjacent to, but isolated from, the magnet ring surface by the thin flexible mica insulator shown in Fig. 1b.

Electrons were supplied to the discharge from a toroidal, thermionic cathode located 1.5 cm upstream of the screen grid so that its axis would be coincident with the discharge chamber axis (Fig. 1a). The major diameter of the cathode torus, d_c could be varied by altering the cathode support post heights. The total length of the 0.25-mm-diam tungsten wire used to fabricate the torus was always the same. It was formed into a spiral coil that was stretched to various extents to produce cathode torus major diameters that ranged from 1 to 6 cm. The ion beam diameter d_b, which could be varied

Received Aug. 15, 1985; presented as Paper 85-0007 at the AIAA/DGLR/JSASS 18th International Electric Propulsion Conference, Alexandria, VA, Sept. 30-Oct. 2, 1985; revision received April 14, 1986.

*Research Assistant, Department of Mechanical Engineering; presently at AT&T Information Systems, Middletown, NJ.

†Professor, Department of Mechanical Engineering. Member AIAA.

by changing the extent to which the screen grid was masked down, was 8 cm unless otherwise noted. The discharge chamber length ℓ_d, which could also be varied, was generally maintained at 11.8 cm. The upstream distance from the screen grid to the ring cusp ℓ_r was 3.7 cm unless otherwise noted. The physical transparencies of the screen and accelerator grids were 0.68 and 0.54, respectively.

In specific tests, the discharge voltage V_D was held constant at 50 V, the argon flow rate $\dot{m}$ was varied over the range 100-700 mA eq., and at each flow rate the discharge current J_D was varied through the range ~0.1 to ~2 A. At each operating condition, the variables just identified, the beam current J_B, and the total ion production rate J_P, were measured. When the movable anode was installed, it was positioned initially at the axial location of the magnetic field cusp produced at the ring magnet ($\ell_a = 0$), and it was then moved downstream after each sequence of data collection. When the anode had been moved too far from the axial location of the magnetic field cusp, the discharge would cease. The axial location of the anode at which this occurred repeatedly for a given anode loop diameter will be referred to herein as the extinction point for that anode loop diameter. More detailed descriptions of the apparatus and procedures used in conducting these tests are presented in Refs. 4 and 5.

The test results will be presented in terms of the parameters describing the energy cost of a plasma ion ϵ_P and the fraction of ions produced that are extracted into the beam f_B. These parameters have been computed from experimental data using the equations[2]

$$f_B = J_B / J_P \tag{1}$$

$$\epsilon_P = (J_D - J_P) V_D / J_P \tag{2}$$

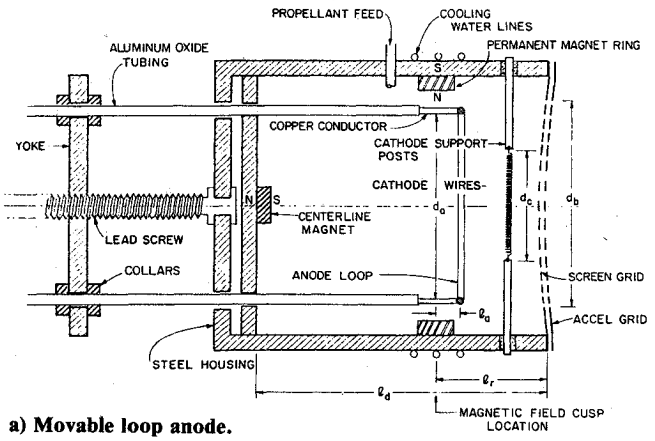

a) Movable loop anode.

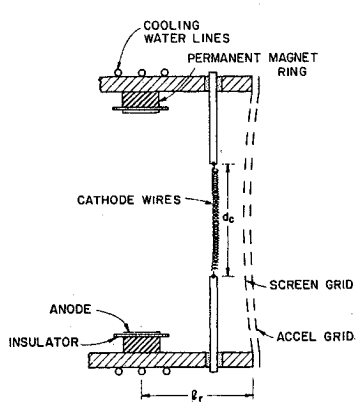

b) Anode on cusp.

Fig. 1 Ion source configurations.

All the quantities appearing on the right-hand sides of these equations except the ion production current were measured directly. The ion production current was measured by biasing the thruster body and screen grid ~30 V negative of cathode potential to repel electrons so that the ion currents to each of these surfaces could be measured. The sum of ion currents to these surfaces and the beam current approaches the total ion production current J_P. (The error between true ion production current and the measured one is due to the collection of ions on the anode and the cathode wires and support posts. This error should be small because the effective collection areas of these surfaces are small compared to the total area exposed to the plasma.[2])

Data will also be presented herein in terms of the neutral density parameter. This parameter, which is proportional to the neutral density in the discharge chamber is defined by the expression $\dot{m}(1-\eta_u)$ where $\dot{m}$ is the propellant flow rate into the thruster and η_u is the propellant utilization efficiency. It has been shown by Brophy[2] that the plasma ion energy cost is related to the neutral density parameter by the equation

$$\epsilon_p = \epsilon_p^* [1 - e^{-C_0 \dot{m}(1-\eta_u)}]^{-1} \tag{3}$$

In this equation the parameter ϵ_p^*, the baseline plasma ion energy cost, is the average energy required to produce an ion at high neutral densities. When the neutral density is sufficiently high, primary electrons are not lost directly to the anode, and the only losses associated with ion production are those related to atomic excitation reactions and Maxwellian electron energy losses to the anode. A more detailed description of the relationship between Maxwellian electron losses and the baseline plasma ion energy cost, including a model for calculating this cost, is contained in Ref. 2. The other parameter contained in Eq. 3, the primary electron utilization factor C_0, is given by the equation

$$C_0 = \frac{4\sigma_0' \ell_e}{e v_0 A_g \phi_0} \tag{4}$$

where σ_0 is the total inelastic collision cross section for primary electron-neutral atom collisions, ℓ_e the primary electron containment length (i.e., the average distance primary electrons would travel in the thruster before reaching the anode if they had no inelastic collisions), e the electron charge, A_g the grid area, ϕ_0 the grid transparency to neutral atoms, and v_0 the mean velocity of the neutral atoms. A higher value of C_0 is indicative of better primary electron containment.

While the plasma ion energy cost and extracted ion fraction are useful in determining the cause-and-effect relationships that are the focus of this work, it is the beam ion energy cost ϵ_B that is of primary concern to a propulsion system designer. This beam ion energy cost is related to the other two parameters through the equation[2]

$$\epsilon_B = \frac{\epsilon_p}{f_B} + \frac{1 - f_B}{f_B} V_D \tag{5}$$

Hence, data presented in the form of plasma ion energy costs and extracted ion fractions can be readily converted into beam ion energy cost data.

Experimental Results

Effect of Anode Axial Position on Plasma Ion Energy Cost

As the anode loop shown schematically in Fig. 1a was moved downstream from the axial location of the magnetic field cusp, the plasma ion energy cost was observed to decrease continuously until it reached a point where the discharge went out. The lowest (optimum) plasma ion energy cost was realized as this threshold of discharge extinction

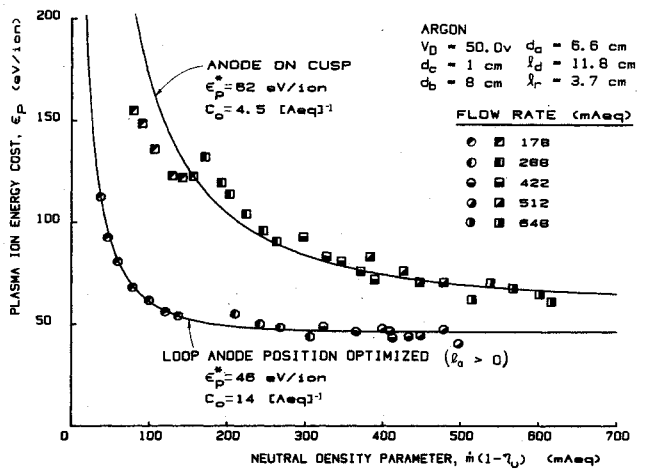

Fig. 2 Typical results showing the effect of anode position on plasma ion energy costs.

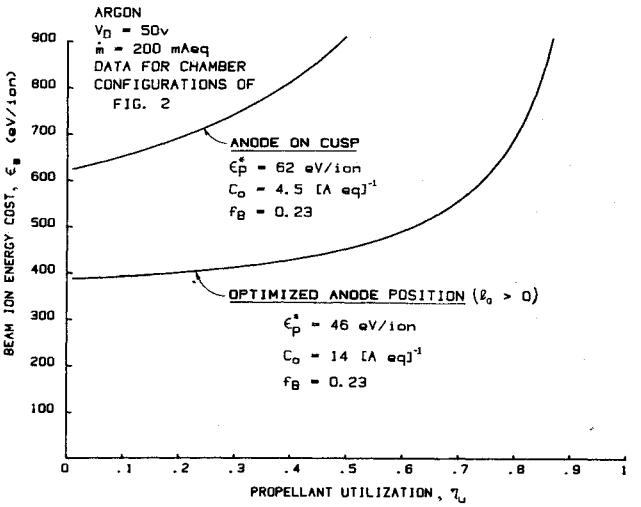

Fig. 3 Typical effect of anode position on thruster performance.

was approached. The extent of the reduction in plasma ion energy costs induced by changing the region of electron collection from the surface of the cusp (configuration of Fig. 1b) to the downstream loop anode location where discharge extinction is approached (configuration of Fig. 2). The parameters associated with each curve shown (ϵ_p^* and C_0) are the ones that correspond to the best fit of Eq. (3) to the data. The higher value of C_0 associated with the optimized anode location data of Fig. 2 reflects a corresponding improvement in the primary electron containment when the anode is positioned properly (specifically, this comes about because of an increase in the primary electron containment length ℓ_e). The lower value of ϵ_p^* observed when the anode loop is in its optimum location is probably due to lower Maxwellian electron energy losses to the anode although it may also reflect reduced ion losses to the anode.

It is noteworthy that the square symbol data of Fig 2, while they do tend collectively to follow the theoretical curve shown, may not follow it well at any one flow rate (e.g., at 178 mA eq.). This tendency to depart from the theory embodied in Eq. (3) as neutral density is reduced at a given flow rate was also observed by Brophy.[2] The departure is believed to be caused by an increase in the average energy of the Maxwellian electrons collected at the anode, which tends to accompany reductions in neutral density (i.e., increases in propellant utilization efficiency) at some operating conditions. Such a change would induce an increase in the value of the parameter ϵ_p^*, which has been held constant to obtain the curves of Fig. 2.

Effect of Anode Position on Extracted Ion Fraction and Beam Ion Energy Cost

It is apparent from Eq. (5) that the extracted ion fraction f_B can have a dominant effect on the beam ion energy cost ϵ_B. In these tests it was found, however, that anode movement from the cusp location to the optimized location did not induce significant changes in the extracted ion fraction. Typically it was found that varying the anode axial location from the position over the cusp to the discharge extinction point and varying flow rates over the range given in Fig. 2 resulted in an extracted ion fraction that remained at $f_B = 0.23 \pm 0.02$. Hence, the minimum beam ion energy cost was realized when the plasma ion energy cost was a minimum (i.e., at the optimized anode location). The extent of the typical performance improvement induced in more traditional performance curves by moving the anode from the cusp to the optimized anode location is shown in Fig. 3. These typical performance curves have been computed using Eqs. (3) and (5), the values of the parameters (ϵ_p^*, C_0) associated with the data of Fig. 2, a mass flow rate of 200 mA eq., and $f_B = 0.23$. Experimental data points are not given in Fig. 3 or other performance curves (ϵ_B vs n_u) appearing in this paper because the focus of the tests was measurement of plasma ion energy cost and extracted ion fractions and control of the many experimental parameters was not always adequate to assure small data scatter on the performance curves. For example, the data of Fig. 2 were collected with toroidal cathodes that had slightly different major diameters. This variation in diameter did not affect the plasma ion energy cost curves, but it did affect the extracted ion fractions. A subsequent test demonstrated the minor effect anode position and flow rate had on extracted ion fraction. The plots of Fig. 3 represent therefore what would be expected if everything but anode position were held constant.

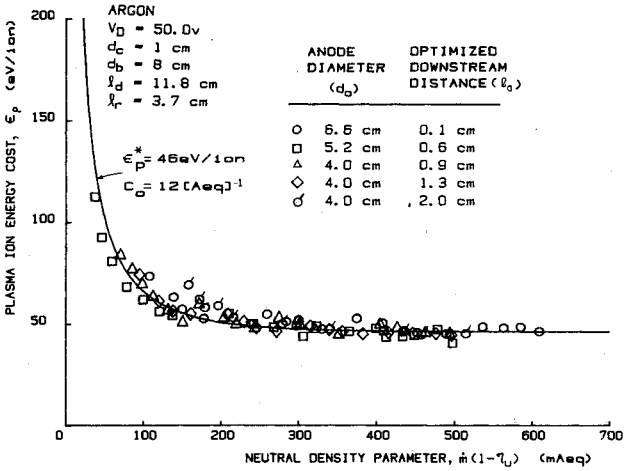

Fig. 4 Effect of anode diameter on plasma ion energy cost curve for anode axial position optimized.

Optimum Anode Locations Relative to the Magnetic Field Lines

A series of tests was was conducted to determine how the optimum anode axial position varied as the anode diameter was changed. With the beam diameter, discharge chamber length, and cathode diameter held as constant as possible, the chamber was operated in three tests, each characterized by an anode loop with a different major diameter. When the anode was moved near the discharge extinction point in each of these three tests, the performance was again observed to be opti-

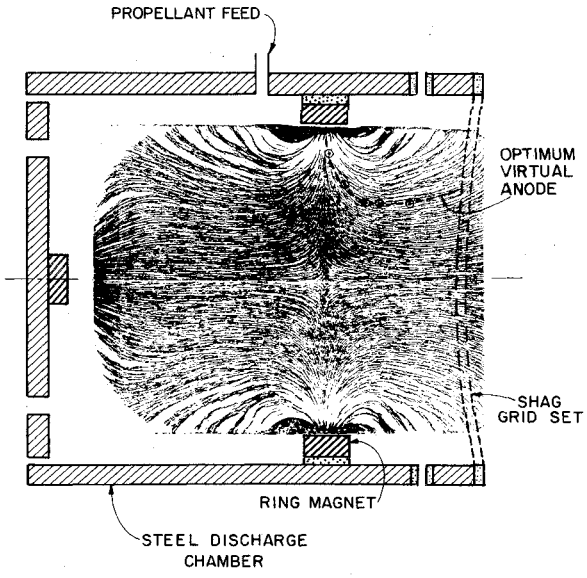

Fig. 5 8-cm-diam ring cusp thruster magnetic field map.

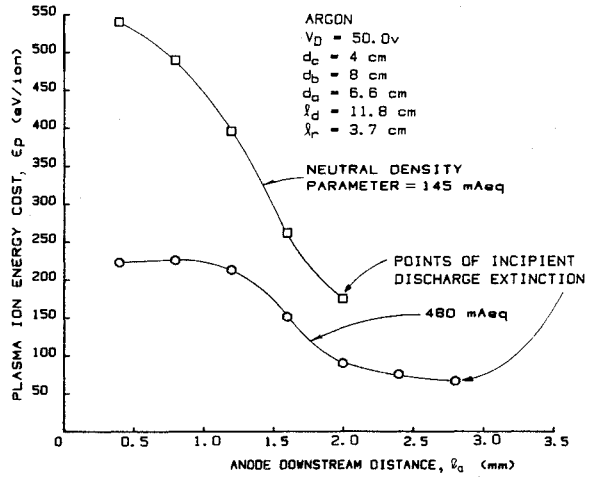

Fig. 6 Effect of anode position and neutral density on plasma ion energy cost.

mized. The most striking feature of the test results, however, was that the resulting plasma ion energy cost/neutral density parameter data points measured at these optimized anode positions fell on a common curve. This curve is shown, along with the data points corresponding to each anode diameter in Fig. 4. The consistency of these data illustrates that proper placement of any anode potential surface within the discharge chamber yields the same optimum discharge chamber performance. This consistency is also reflected in the parameters C_0 and ϵ_p^* used to define the curve fit of the separate sets of data in Figs. 2 and 4. The values of these parameters are observed to agree exactly in the case of ϵ_p^* and to within $\pm 10\%$ in the case of C_0. It is noteworthy that for the 4-cm-diam anode, the performance remained at the same high level as the anode was moved through a rather large range of axial positions (0.95 cm $\leq \ell_a \leq 2.0$ cm).

Some insight into why the locations of the anode loop identified in Fig. 4 yield this optimum performance can be gained by plotting the optimum anode loop positions on the iron filings map of the magnetic field shown in Fig. 5. This iron filings map was made using a new technique[4] developed for high-field-strength, permanent magnet ion thrusters. Careful examination of these anode locations suggests that to first order they fall along a common magnetic field line. Since performance was optimum for each of the anode positions plotted in Fig. 5, these positions lie along the optimum virtual anode field line and its surface of revolution would represent the optimum surface for collecting electrons.[6] In more general terms, one can say that the same performance is achieved in a discharge chamber for an anode positioned to collect electrons at any place along the surface of revolution of a given virtual anode field line and that this performance is optimized when this field line is properly selected.

The effect of the alignment between the directions of anode motion and of the magnetic field lines on the distance over which the anode could be moved without inducing substantial changes in the plasma ion energy cost is illustrated by the data in the legend of Fig. 4. These data show that the 4-cm-diam anode loop could be moved axially for more than 1 cm and, because it was moving along the optimum virtual anode field line (Fig. 5), the plasma ion energy cost remained essentially constant. With the 6.6-cm-diam anode loop in place, however, axial movement was essentially normal to the field lines (Fig. 5), and a mere 0.5-mm upstream movement from the location of discharge extinction caused substantial increases in plasma ion energy costs. A preferred anode diameter (i.e., one that is least sensitive to anode axial position) was for this experiment, therefore, one that allowed the anode loop to move along the optimum, virtual anode field line at the location where this field line ran parallel to the axis of the discharge chamber.

As the anode loop was moved downstream during typical investigations of anode position on performance, it was observed that on some occasions the plasma ion energy cost was decreasing dramatically as the point of discharge extinction was approached. On other occasions it was found that the anode could be moved over a substantial distance with no significant change in plasma ion energy cost. The distance over which the anode could be moved toward the point of discharge extinction with no substantial change in plasma ion energy cost was observed to be a function of both the neutral atom density and the extent to which the anode was being moved along magnetic field lines. Typical results showing the effect of the neutral density parameter on the range of anode positions over which the plasma ion energy cost remained nearly constant can be seen in Fig. 6. Here the plasma ion energy cost is plotted against anode position (measured downstream from the cusp location). At a neutral density parameter of 145 mA eq., the curve drawn through the square data symbols shows a very sharp drop in the plasma ion energy cost as the anode loop is moved downstream of the magnetic ring cusp. In this case the discharge could not be sustained with the anode loop positioned beyond the 2-mm downstream position. Operating at a neutral density parameter of 480 mA eq. did, however, make it possible to vary the anode loop position through a range of about 1 cm while achieving approximately the same plasma ion energy cost. This increase in the range of acceptable anode positions is apparently related to an increase in the collision frequency of electrons with neutral atoms in the discharge plasma. This is presumably related in turn to the fact that an increased collision frequency facilitates electron migration across field lines.

An analytical criterion that can identify the magnetic field line that defines the optimum virtual anode field line would be desirable. Research conducted to date gives some insight into the formulation of such a criterion. This research has shown that the position of this line should be measured relative to the position of the outermost magnetic field line that can receive primary electrons directly from the cathode. It should be noted that electrons from the cathode can migrate along magnetic fields within the discharge chamber with relative ease, and they can also migrate inward where there is no anode to collect them and where magnetic fields are weaker. Electrons released from the cathode should therefore fill the region within the surface of revolution of the magnetic field line that intersects the outer edge of the

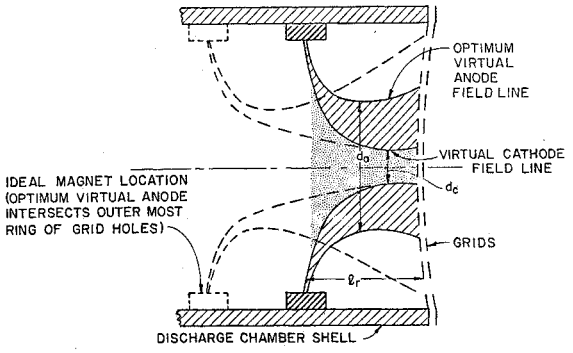

Fig. 7 Schematic diagram of important magnet field lines.

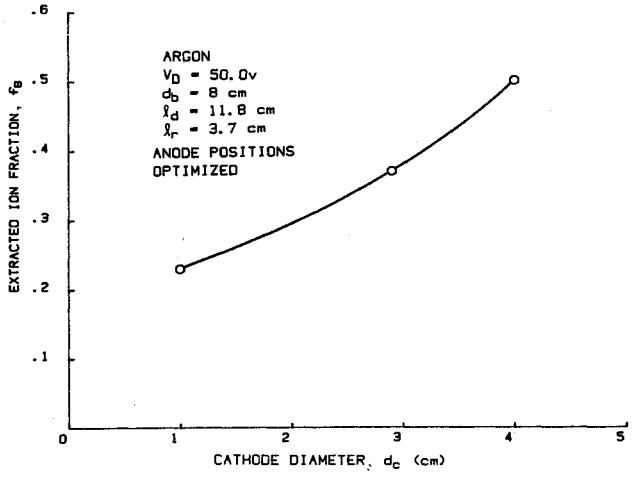

Fig. 8 Effect of cathode diameter on extracted ion fraction.

cathode. This field line, which will be called the virtual cathode magnetic field line herein, has also been labeled the critical magnetic field line.[7] Figure 7 is an illustration showing the selected magnetic field lines within the discharge chamber that have just been defined. Primary electrons emitted from the cathode with diameter d_c would have access to the dotted region shown, which is bounded by the solid virtual cathode field lines. These electrons would migrate through the crosshatched region toward the optimum virtual anode field lines where they would be collected, usually as Maxwellian electrons. If these two field lines were too close together, then significant numbers of primary electrons would reach the virtual anode and be lost, and high plasma ion energy cost would result. If, on the other hand, the virtual anode and cathode field lines were too far apart, the discharge would tend to extinguish. An example of a criterion that might be used to define an acceptable separation distance between the virtual field lines is the magnetic field integral criterion suggested by Robinson.[8]

Effect of Ring Cusp Location on Performance

Based on the model just discussed, ionization may be presumed to occur within the region bounded by the optimum virtual anode field lines of Fig. 7. For the magnetic field line configuration designated by the solid field lines of Fig. 7, this implies that the ion production region (dotted and crosshatched) does not extend to the outer ring of holes in the grid set and that the ion beam profile would be peaked. It might be postulated that this situation could be corrected by moving the ring magnet upstream and repositioning the anode onto the new optimum virtual anode line. The optimum virtual anode and the virtual cathode field lines that might be expected in this situation are shown as dashed lines in Fig. 7. In order to test this hypothesis, a test was run in which the ring cusp/screen grid separation

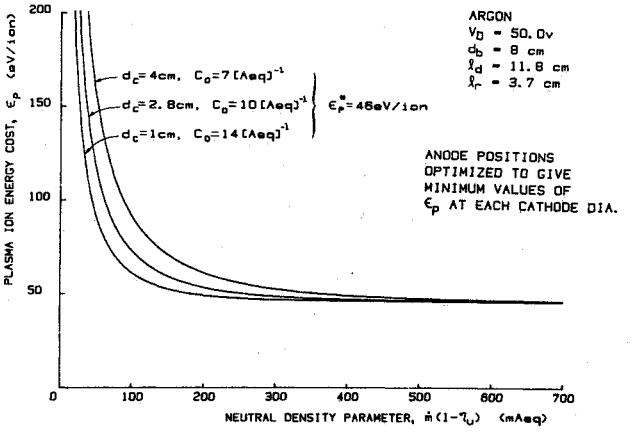

Fig. 9 Effect of cathode diameter on plasma ion energy cost.

distance ℓ_r was increased from the standard value (3.7 cm) to 4.5 cm. The results, which confirmed the hypothesis, showed that this change induced an increase in the extracted ion fraction from 23 to 33%. Further, an iron filings map taken with ℓ_r equal to 4.5 cm suggested, qualitatively at least, that the optimum virtual anode field lines shown dashed in Fig. 7 were realized.

Effect of Cathode Diameter on Performance

The cathode diameter d_c could also be increased to alter the ion production region from that shown in Fig. 7 so that both the ion beam profile and extracted ion fraction would be improved. The anode would also have to be repositioned onto the new optimum virtual anode field line, in this case to keep the plasma ion energy cost at its optimum level. The effect of cathode diameter on extracted ion fraction for the case where the anode position was readjusted to yield minimum plasma ion energy costs is shown in Fig. 8. These data were obtained at the discharge chamber configuration defined by Fig. 1a, with the chamber configured to have the lengths and diameters cited in the legend of Fig. 8. These data show that the extracted ion fraction more than doubles as the cathode diameter d_c is increased from 1 to 4 cm. This improvement in the extracted ion fraction is believed to be caused in part by an increase in the grid area exposed to the primary electron plasma and in part by an increase in the fraction of the total ion production effected adjacent to the grids.

Increasing the diameter of the cathode has the adverse effect of increasing plasma ion energy costs, as the curves of Fig. 9 illustrate. The actual data points on which these curves are based are not shown in this figure because there were a large number of them and they tend to complicate the figure without providing significant additional information. The increase in plasma ion energy cost induced by increases in cathode diameter is shown in Fig. 9 to be relatively modest at low propellant utilization levels (high neutral density parameters). This is shown by the fact that increasing the cathode diameter from 1 to 4 cm leaves the baseline plasma ion energy cost unchanged. This change in cathode diameter is, however, observed to cause the primary utilization factor C_0 to decrease. Lower primary electrons utilization factors imply less effective containment of the primary electron in the discharge until after they have had inelastic collisions [Eq. (4)]. This leads to the conclusion that larger-diameter cathodes induce a larger primary electron loss rate to the anode. Fortunately, the improvement in the extracted ion fraction f_B induced by increasing the cathode diameter outweighs the effect of the reduced primary electron utilization factor C_0. As a result, the overall performance of the discharge chamber is greatly improved by increases in

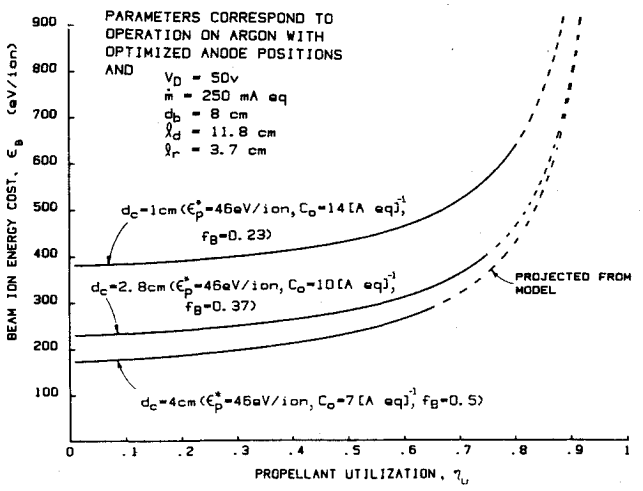

Fig. 10 Effect of cathode diameter on thruster performance.

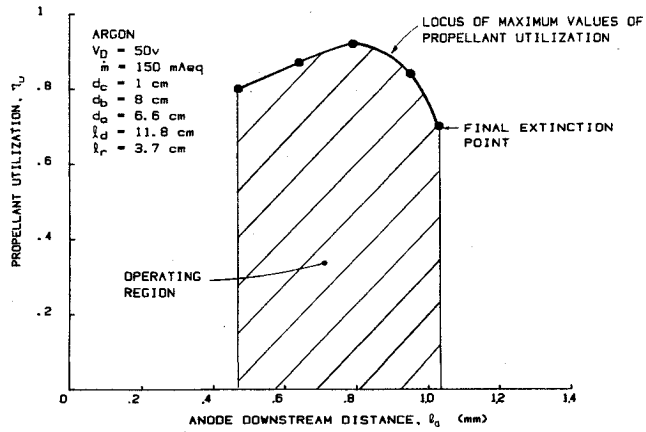

Fig. 11 Typical effect of anode position on propellant utilization range.

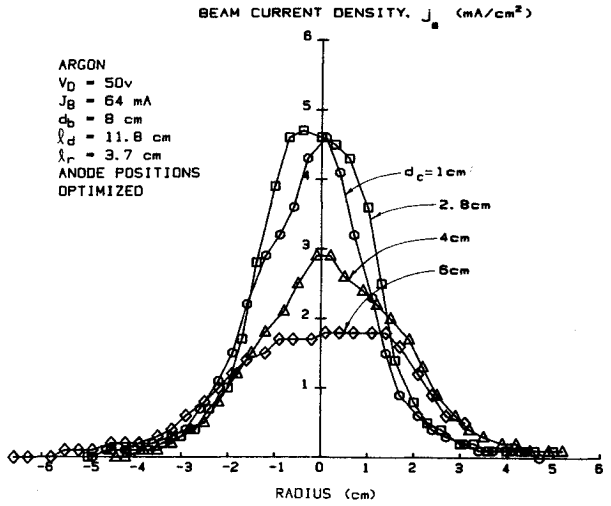

Fig. 12 Effect of cathode diameter on ion beam profile.

cathode diameter. This is shown by the plots of Fig. 10, which present performance curves computed using Eqs. (3) and (5) and the curve fit values of the parameters f_B, ϵ_p^* and C_0, identified in Figs. 8 and 9. Specifically, they illustrate the dramatic improvement in performance achieved as cathode diameter d_c is increased from 1 to 4 cm and as f_B, the extracted ion fraction, increases from 23 to 50%. The measured data are in agreement with the curves of Fig. 10 up to the dashed lines, at which point the discharge could no longer be sustained at each particular operating condition. The dashed lines do, however, represent the performance projected by the model [Eqs. (3) and (5)] at higher propellant utilizations.

The limitations on propellant utilization that prevented operation at values indicated by the dash lines in Fig. 10 were due primarily to the fact that the anode loop was located too close to the final discharge extinction point. This limitation was mentioned in discussing Fig. 6, but it is described in more general terms by the data of Fig. 11. This figure shows a typical plot of the propellant utilization n_u against the anode downstream distance ℓ_a measured at the particular condition defined in the legend. The figure shows that operation near the final extinction point, where the plasma ion energy costs are lowest, limits the maximum propellant utilization to approximately 70%, while operation with the anode loop positioned 2 mm further upstream, where the plasma ion energy costs are only slightly higher, makes it possible to achieve propellant utilizations greater than 90% before discharge extinction occurs. This observation suggests that the optimum anode location for a given discharge chamber will involve a compromise between the maximum propellant utilization and the minimum plasma ion energy cost.

The operating range of the thruster seems to be limited at the left-hand boundary of the crosshatched region of Fig 11 by excessive primary electron losses to the anode (i.e., many primary electrons go directly to the anode without having Maxwellian electron-producing collisions). It is postulated that such losses reduce the electron density to the point where the required total anode current (i.e., that due to both primary and Maxwellian electrons) cannot be sustained at the prevailing discharge voltage. On the right-hand boundary, the thruster operation seems to be limited because the conductivity of the plasma between the virtual anode and cathode field line surfaces becomes too low and the demanded discharge current cannot be conducted with the available potential difference. It should be noted that the data of Fig. 11 were obtained at a 150 mA eq. flow rate and that the range of anode downstream distances and propellant utilizations over which operation can be sustained increases with flow rate.

The cathode diameter was also found to affect the ion beam profile of this 8-cm-diam ring cusp thruster. Beam profile data measured at a 64-mA beam current for four different cathodes with diameters varying from 1 to 6 cm are plotted in Fig. 12. Each of these curves integrates to yield the measured beam current to within several percent. The flatness parameter corresponding to each curve in Fig. 12 is plotted against the cathode diameter in Fig. 13. This figure shows that increasing the diameter from 1 to 4 cm results in a modest improvement in the flatness parameter, while the change in d_c from 4 to 6 cm results in a more substantial improvement. Since a flatter beam profile must be induced by a flatter plasma density profile in the discharge chamber,[9,10] increasing the cathode diameter must improve the discharge plasma uniformity at the grids.

Effect of Discharge Chamber Length

Changing the locations of the virtual cathode and virtual anode magnetic field lines by changing the anode and cathode positions has been shown to affect substantially the overall performance of an 8-cm-diam ring cusp thruster. Changing the discharge chamber length, however, had no effect on the plasma ion energy cost and only a minor effect on the fraction of ions extracted into the beam. The discharge chamber performance plot of Fig 14 illustrates this insensitivity of the performance data to changes in the discharge chamber length over the range of values from 5.3

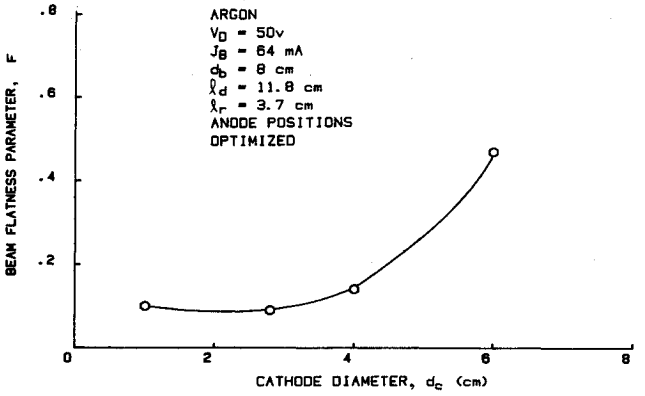

Fig. 13 Effect of cathode diameter on ion beam flatness parameter.

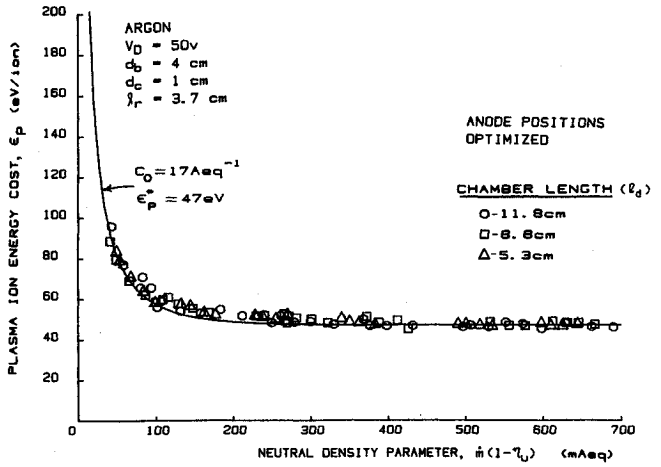

Fig. 14 Effect of discharge chamber length on plasma ion energy cost curve—anode axial position optimized.

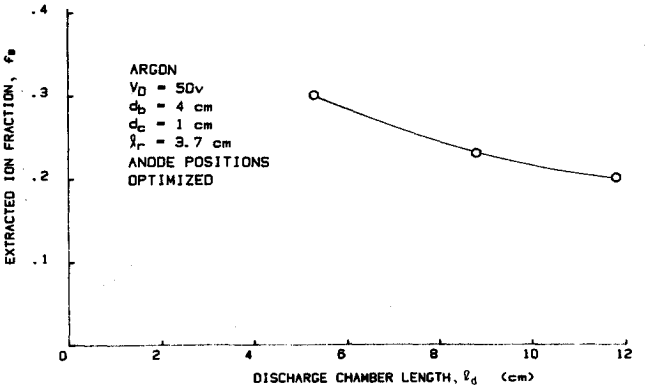

Fig. 15 Effect of discharge chamber length on extracted ion fraction.

to 11.8 cm. For each chamber length, the anode loop location was optimized as described earlier and, although the optimum anode position for each chamber length was different, the plasma ion energy cost data at a given neutral density remained unchanged. It should be noted that the relatively high value of the primary electron utilization factor $C_0 \approx 17$ A eq.$^{-1}$ is due primarily to the masked-down grid ($d_b = 4$ cm) used in this particular test and that an even higher value would be expected based on the data of Fig. 4 and Eq. (4). This equation suggests that halving the grid area would quadruple C_0 which would imply a C_0 of ~48 for the data of Fig. 14. The reason the C_0 for Fig. 4 is not this large is unclear, but it is believed to be related to the small thruster

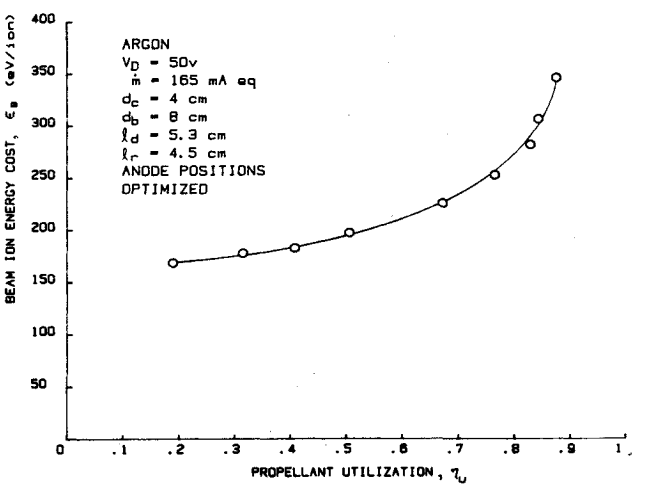

Fig. 16 Optimized performance curve for 8-cm-diam ring cusp thruster.

size and the plasma nouniformity that exists in such a thruster. In a larger, 15-cm-diam thruster, Brophy[2] did observe the changes in C_0 with beam diameter predicted by Eq. (4).

While shortening the discharge chamber length does not change the plasma ion energy cost curves, it does increase the extracted ion fraction. This improvement in f_B, which may have been caused by the altered magnetic field shape upstream of the magnetic ring cusp and/or the reduction in the total area to which ions in the discharge plasma could be lost, is shown in Fig. 15. It should be noted that, while the data of Fig. 15 were obtained at a neutral density parameter of 150 mA eq., the extracted ion fraction is independent of neutral density,[2] so that these data may be taken as typical. In fact, it was observed in collecting the data for Figs. 14 and 15 that the extracted ion fraction varied less than 2% as the neutral density parameter was varied over the full range investigated at any discharge chamber length.

Overall Performance Optimization

In order to optimize the overall performance of the 8-cm-diam ring cusp thruster studied here, it has been shown that certain geometrical relationships should be satisfied. These relationships, which are admittedly incomplete at this time, should eventually lead to a theoretical discharge chamber model that would enable a designer to specify the optimum geometry of a thruster without resorting to experimental optimization procedures. In conducting the experiments described herein, the relationships have been investigated by varying such parameters as cathode diameter, anode position, and discharge chamber length, but variations in these parameters are viewed most logically in terms of the critical magnetic field lines they define. If one begins at the grids, where the beam diameter is defined, rather than with an arbitrarily positioned cathode, where the experimental investigation began, the logical sequence of guidelines is the following:

1) The anode should be positioned in the magnetic field so that the virtual anode field line intersects the outermost ring of holes in the screen grid. This condition helps to assure a maximum extracted ion fraction and a flat ion beam profile.

2) The filament cathode diameter d_c should be selected so that the associated virtual cathode field line is separated from the virtual anode field line by an amount that will assure that this latter field line behaves as the optimum virtual anode that yields low plasma ion energy costs. While the criterion that determines the separation between the virtual anode and cathode field lines has not been quantified, it is believed to be related to the line integral of the magnetic field intensity along a line orthogonal to the field lines.[6] It is

known that the plasma ion energy decreases as the separation distance between these field lines is increased up to the point where the discharge goes out. It is believed that the plasma ion energy cost decreases as the separation between the virtual anode and cathode field lines is increased because of improved primary electron containment.

Two additional discharge chamber parameters that were varied in these tests and had less significant effects on performance were the following:

1) Reducing the discharge chamber length ℓ_d from 1.5 times its diameter to 0.7 times its diameter induced a monotonic increase in the extracted ion fraction. Mechanical interference problems prevented further reductions in length so that it could not be determined if this trend continued to shorter chamber lengths.

2) Increasing the distance between the ring cusp and the screen grid ℓ_r from 3.7 to 4.5 cm induced an increase in the extracted ion fraction. Increasing this distance would be expected to change the magnetic field shape and intensity in the vicinity of the grids. It is believed that increasing this distance tends to reduce the magnetic field strength near the grids and thereby improve the uniformity of both the magnetic field and the plasma density at the grids. It should be noted at this point that the problems of magnetic field shaping and radial plasma uniformity near the grids are much more severe in the 8-cm-diam ion source used in this study than they would be in larger ones (e.g., 15 or 30-cm-diam thrusters).

In order to test the preceding design guidelines, they were applied to define a discharge chamber geometry for the 8-cm-diam ring cusp thruster that would be expected to yield good performance curves. A typical example of a resulting performance curve (measured at a flow rate of 165 mA eq.) is shown in Fig. 16.This performance curve is considered exceptionally good for a small, 8-cm-diam ion source being operated on argon.

Finally, it is noted that while the anode diameter could be selected to have any value that would enable it to be located on the virtual anode field line, it is probably preferable for it to have a value equal to the diameter of the virtual anode field line in the region where it is parallel to the thruster axis. At this condition the performance and discharge stability were observed to be relatively insensitive to the axial location of the anode.

Conclusions

The efficiency of an 8-cm-diam chamber having one centerline and one ring magnetic field cusp is improved substantially by moving the electron collection surface (anode) from the magnetic cusp surface to a location downstream of the ring cusp. In its preferred position the anode establishes contact with a circle on the surface of revolution of the optimum virtual anode magnetic field line. With the anode at this position, the discharge is close to the point of extinction, but plasma ion energy costs are minimized because primary electron losses to the anode are low. No change in the fraction of ions extracted into the beam is observed when the anode is moved from the magnetic cusp surface to the optimum virtual anode field line. These observations lead one to conclude that Sovey[3] could have achieved even better performance in his 30-cm-diam ring cusp discharge chamber if he had located his anodes away from the magnet surfaces rather than on them.

Changing the diameter of a circular cathode surface supplying primary electrons to the discharge also influences discharge chamber performance, but it does so primarily because it influences the position of the optimum virtual anode. When the cathode is positioned so that the optimum virtual anode field lines intersect the outermost ring of holes in the screen grid, the preferred condition of a high extracted ion fraction will be achieved. The extracted ion fraction can also be increased by decreasing the discharge chamber length. With the anode located so that it is in contact with a circle on the surface of revolution of the optimum virtual anode field line, no change in the plasma ion energy cost is observed as the chamber length is changed. A slight increase in the plasma ion energy costs accompanies increases in cathode diameter. The best overall operating condition is observed when the cathode and anode positions and the magnetic field configuration are selected so that the discharge operates stably near the discharge extinction point and the optimum virtual anode field line intersects the outer ring of holes in the grid system.

Acknowledgment

This work was supported by NASA Lewis under Grant NGR-06-002-112.

References

[1]Brophy, J. R. and Wilbur, P.J., "The Flexible Magnetic Field Thruster," *Journal of Spacecraft and Rockets,* Vol. 20, Nov.-Dec. 1983, pp. 611-618.

[2]Brophy, J.R., "Ion Thruster Performance Model," NASA CR-174810, Dec. 1984.

[3]Sovey, J.S. "Improved Ion Containment Using a Ring-Cusp Ion Thruster," AIAA Paper 82-1928, Nov. 1982.

[4]Wilbur, P.J., "Advanced Ion Thruster Research," NASA CR-174862, Jan. 1985, pp. 5f and 56.

[5]Hiatt, J. M. and Wilbur, P. J., "Ring Cusp Discharge Chamber Performance Optimization," AIAA Paper 85-2007, Oct. 1985.

[6]Longhurst, G.R. and Wilbur, P.J., "Plasma Property and Performance Prediction for Mercury Ion Thrusters," *Progress in Astronautics and Aeronautics: Electric Propulsion and Its Application to Space Missions,* Vol. 79, AIAA, New York, pp. 224-250.

[7]King, H.J. et al., "2½ kw Low Specific Impulse, Hollow Cathode Thruster," AIAA Paper 69-300, March 1969.

[8]Robinson, R.S., "Physical Processes in Directed Ion Beam Sputtering," NASA CR-159567, March 1979, pp. 14-20.

[9]Wilbur, P.J., " Correlation of Ion and Beam Current Densities in Kaufman Thrusters," *Journal of Spacecraft and Rockets,* Vol. 10, Sept 1973, pp. 623-624.

[10]Beattie, J.R. and Wilbur, P.J., "Cusped Magnetic Field Mercury Ion Thruster," NASA CR-135047, July 1976.